

## STATE-SELECTIVE SPECTROSCOPIC DETECTION OF REACTION PRODUCTS ( $\text{SiH}_2$ , Si) IN THE IR LASER DECOMPOSITION OF $\text{SiH}_4$

Elisabetta BORSELLA and Roberta FANTONI

*ENEA, Dipartimento TIB, U.S. Fisica Applicata, Centro Ricerche Energia Frascati, C.P. 65, 00044 Frascati, Rome, Italy*

Received 19 May 1988; in final form 23 June 1988

The decomposition mechanism of  $\text{SiH}_2(^1\text{B}_1)$  formed after IR multiple-photon dissociation of  $\text{SiH}_4$  has been investigated by simultaneous acquisition of spontaneous chemiluminescence of  $\text{SiH}_2$  radicals and state-selective two-photon laser-induced fluorescence spectra of the atomic silicon produced. Evidence for the opening of an efficient dissociation channel leading to  $\text{Si}(^1\text{D}_2) + \text{H}_2(^1\Sigma_g^+)$  from high vibrational levels of the  $\text{SiH}_2(^1\text{B}_1)$  state is presented and discussed.

### 1. Introduction

It is now well established that silylene ( $\text{SiH}_2$ ) is a key intermediate in a wide range of decomposition processes of silicon hydrides including pyrolysis [1], chemical vapour deposition [2,3], glow discharge [4] and IR laser-induced dissociation [5-7]. It was already suggested [5] that the major feature which differentiates the gas-phase reaction sequences following the initial step



is the energy state in which the radical  $\text{SiH}_2$  is formed. Whenever silylene is formed in the  $^1\text{A}_1$  ground state, its insertion into undissociated  $\text{SiH}_4$  giving rise to higher silanes is the dominant mechanism following step (1) [1]. Otherwise, silicon formation, followed by particle nucleation and condensation, is observed when  $\text{SiH}_2$  is formed in the electronic excited  $^1\text{B}_1$  state [5]. It was also recently observed [8,9] that the gas-phase reaction dynamics following the primary step (1) changes depending on the degree of vibrational excitation of the  $^1\text{B}_1$  electronic state. In fact, at  $v_2' \leq 7$  the  $^1\text{B}_1$  state may couple to the triplet surface ( $^3\text{B}_1$ ) and tunnel through the potential barrier to form  $\text{Si}(^3\text{P}) + \text{H}_2$ . A more efficient direct dissociation of  $\text{SiH}_2$  to  $\text{Si}(^1\text{D}_2) + \text{H}_2$  is allowed from  $v_2' > 7$  bending vibrational levels of the  $^1\text{B}_1$  state.

The aim of this paper is to investigate the process of  $\text{SiH}_2$  dissociation leading to atomic silicon pro-

duction after the IR MPD (multiple photon dissociation) of silane. Interest in the subject is primarily due to the importance of silane as starting material for the laser-induced formation of thin silicon films [10] and silicon-containing ceramic powders [11,12].

In order to understand the decomposition dynamics of  $\text{SiH}_2$  following IR MPD of silane, we monitored the formation of gas-phase  $\text{Si}(^3\text{P}$  and  $^1\text{D}_2)$  atoms by laser-induced fluorescence (LIF) and detected the simultaneous visible emission from undissociated electronically excited  $\text{SiH}_2$  fragments.

### 2. Experimental

Silane (99.999% pure, supplied by L'Air Liquide) was excited using a pulsed multimode, line-tunable TEA  $\text{CO}_2$  laser (Lumonics model 203). A typical pulse shape consisted of a 150 ns (fwhm) peak followed by a tail of 1.5  $\mu\text{s}$ . Laser energy was monitored by collecting on the surface of a Gen-Tec pyroelectric detector (model PRJ-D) a fraction of the laser beam which was deflected by a 10% reflectivity ZnSe beam splitter. Whenever necessary, the pyroelectric detector was replaced by a fast detector (Molelectron model P3) in order to obtain the IR laser pulse time profile. The laser beam was mildly focused in the centre of the cell by a 1.5 m focal length spherical copper mirror which produced a collimated region of radiation

along the cell axis. The beam cross section, as measured by burnt patterns on thermosensitive paper, was  $0.22 \text{ cm}^2$  in the centre of the empty cell. Typical laser fluences were in the range  $1\text{--}8 \text{ J/cm}^2$ .

The cell was a UHV stainless steel six-way cross equipped with two ZnSe windows for  $\text{CO}_2$  laser transmission and quartz (suprasil) windows for visible-UV light collection and transmission. Conical light baffles were inserted in the cell in order to minimize scattered dye laser radiation and to prevent  $\text{CO}_2$  laser produced powders from reaching (and fogging) the optical windows. A background pressure lower than  $10^{-5}$  Torr was achieved by evacuating the cell with a turbomolecular pump (Elettrorava model ETP 8/450).

State-selective silicon atom detection was accomplished using two-photon LIF. Energy states relevant to the detection of  $\text{Si}(^3\text{P}_J)$  and  $\text{Si}(^1\text{D}_2)$  have been reported by Brewer [13]. A LIF signal in the range  $250.7\text{--}252.8 \text{ nm}$  from  $^3\text{P}_0^o$  states is expected after two-photon excitation of  $\text{Si}(3^3\text{P}_{J'}) \rightarrow \text{Si}(4^3\text{P}_J)$  transitions in the range  $405\text{--}412 \text{ nm}$ ; LIF signals at  $243.51 \text{ nm}$  (from the  $3^1\text{D}_2^o$  state) and at  $288.16 \text{ nm}$  (from  $4^1\text{P}_1^o$ ) follow two-photon excitation of  $\text{Si}(3^1\text{D}_2)$  to  $\text{Si}(4^1\text{D}_2)$  at  $455.67 \text{ nm}$  [13]. Silicon transitions were excited by the tunable radiation emitted from a XeCl (Lambda Physik EMG 103 MSC) pumped dye laser (Lambda Physik model FL 2002). The dye laser radiation ( $2\text{--}3 \text{ mJ}$  energy/pulse;  $\approx 12 \text{ ns}$  pulse duration;  $\approx 0.2 \text{ \AA}$  bandwidth) entered the cell at right angles to the  $\text{CO}_2$  laser beam through a suprasil window after passing a  $15 \text{ cm}$  focal length quartz lens.

The LIF signal was collected at right angles to both laser beams on a RCA 1P28 photomultiplier tube. Appropriate band-pass filters were used to discriminate Si atom fluorescence signals against the scattered radiation from the dye laser. The LIF signal from the photomultiplier output was fed into an EG&G ORTEC fast preamplifier (model 9301), collected on an EG&G boxcar averager (model 162) combined with an EG&G gated integrator (model 165) and displayed on a strip chart recorder.

Synchronization between the  $\text{CO}_2$  and the dye laser was achieved by using a delay generator; a typical delay of  $250 \text{ ns}$  was used throughout the course of this experiment.

$\text{SiH}_2$  visible luminescence was simultaneously detected (at right angles to the  $\text{CO}_2$  laser beam) through

an additional quartz window suitably placed at  $3 \text{ cm}$  from the entrance window of the  $\text{CO}_2$  laser. A  $12.5 \text{ cm}$  focal length quartz lens ( $5 \text{ cm}$  diameter) collected a portion of this radiation and imaged it (with lateral magnification 1) onto the entrance slit of a  $0.32 \text{ m}$  focal length ISA spectrograph (model HR-320,  $f_N=5$ ) supplied with a  $150$  grooves/mm grating. An EG&G optical multichannel analyzer (OMA III) was employed for detection of the  $\text{SiH}_2$  luminescence spectrum. An intensified silicon photodiode array detector ( $512$  elements) was mounted at the exit of the spectrograph and the luminescence spectrum was acquired with a resolution of  $\approx 5 \text{ \AA}$ /channel. An EMI 9658R photomultiplier tube replaced the OMA for time analysis of  $\text{SiH}_2$  luminescence signals. The photomultiplier output was fed into a TEK 2430 digital oscilloscope ( $40 \text{ MHz}$  bandwidth) for signal acquisition and averaging.

The crystalline structure and composition of the  $\text{CO}_2$  laser produced powders were evaluated using X-ray ( $\text{Cu K}\alpha$ ) diffraction analysis [12].

### 3. Results and discussion

Silane (at  $20$  Torr pressure) was irradiated with the output of the TEA  $\text{CO}_2$  laser tuned at  $994.19 \text{ cm}^{-1}$  in the fluence range  $1\text{--}3 \text{ J/cm}^2$ . Over the whole laser fluence interval a powdery silicon deposit is observed inside the cell and a broad spontaneous luminescence spectrum is detected in the wavelength range  $400\text{--}880 \text{ nm}$  (fig. 1). In a previous paper [5], this emission was ascribed to decay from electronic excited states of silylene radicals formed after the IR MPD of  $\text{SiH}_4$ .

The band peaking at  $720 \text{ nm}$  was firmly assigned to the  $^1\text{B}_1 \rightarrow ^1\text{A}_1$  transition, while a proper spectral analysis of the band peaking at  $840 \text{ nm}$  was impossible due to the lack of spectroscopic data for other  $\text{SiH}_2$  electronic excited states. We note that the intensity of the  $\text{SiH}_2$  luminescence increases with laser fluence until a sudden drop (by about a factor of 3) is found when the  $\text{CO}_2$  laser fluence  $\phi$  reaches  $2.5 \text{ J/cm}^2$ , as shown in fig. 1. This decrease in the luminescence spectral intensity is accompanied by a narrowing in the time profile of the emission signal, as shown in fig. 2, and by a relevant increase in the

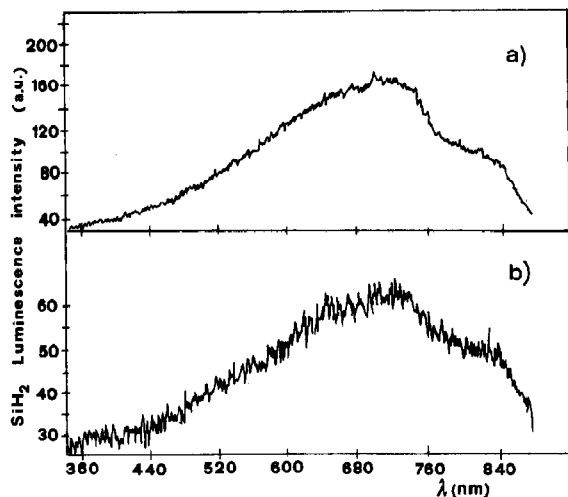


Fig. 1. OMA spectra of  $\text{SiH}_2$  fragment emission after the IR MPD of  $\text{SiH}_4$  at  $p=20$  Torr: (a)  $\phi \approx 2.0 \text{ J/cm}^2$ , (b)  $\phi \approx 2.6 \text{ J/cm}^2$ .

amount of silicon powder produced during the  $\text{CO}_2$  laser irradiation.

Gas phase silicon formation in the ground state has been detected by two-photon LIF exciting the transitions  $3^3\text{P}_{J''}$  ( $J''=0, 1, 2$ ) to  $4^3\text{P}_{J'}$  ( $J'=0, 1, 2$ ) in the range 405–412 nm and observing the group of transitions from  $4^3\text{P}_0^*$  ( $J=0, 1, 2$ ) to  $3^3\text{P}_{J''}$  ( $J''=0, 1, 2$ ) states in the range 250.7–252.8 nm [13,14]. A portion of the LIF excitation spectrum for the  $\text{Si}(^3\text{P})$  atoms, at wavelengths corresponding to the strongest two-photon excitation transitions, is reported in fig. 3. The LIF signal, at 408.45 nm excitation wave-

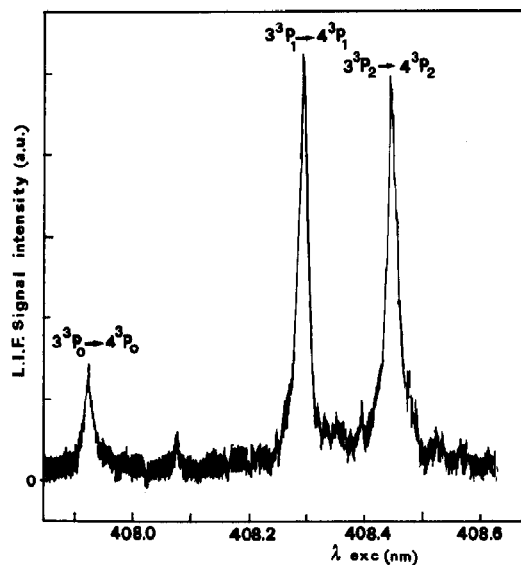


Fig. 3. Two-photon LIF excitation spectrum for  $\text{Si}(^3\text{P}_{J'})$  atoms after IR MPD of  $\text{SiH}_4$  ( $p=20$  Torr) at a  $\text{CO}_2$  laser fluence  $\phi \approx 2.0 \text{ J/cm}^2$ . Only the strongest transitions ( $3^3\text{P}_{J''} \rightarrow 4^3\text{P}_{J'}$  with  $|J'' - J'| = 0$ ) are reported.

length, is reported in fig. 4 for two different  $\text{CO}_2$  laser fluences together with the corresponding  $\text{SiH}_2$  spontaneous emission signals. It appears clearly from data shown in fig. 4 that the change in  $\text{SiH}_2$  chemiluminescence at  $\text{CO}_2$  laser fluences greater than  $2.5 \text{ J/cm}^2$  corresponds to a decrease in the LIF signal from  $\text{Si}(^3\text{P})$  atoms.

Regarding the influence of the  $\text{CO}_2$  laser fluence  $\phi$  on the time dependence of  $\text{SiH}_2$  spontaneous emission reported in fig. 2, we can observe the following. At  $\phi \leq 2.5 \text{ J/cm}^2$ , the time profile of  $\text{SiH}_2$  luminescence signals is mainly determined by energy pooling [15] between vibrationally excited  $\text{SiH}_4$  molecules which provide a continuous source of  $\text{SiH}_2$  emitting fragments until vibrational cooling of the parent molecules is achieved by V-T transfer processes [5]. The sudden decrease of the luminescence decay time at  $\phi > 2.5 \text{ J/cm}^2$  is indicative of the onset of a process which rapidly removes a portion of the emitting fragments.

All these experimental findings lead us to hypothesize the opening of a new dissociation channel to atomic silicon for  $\text{SiH}_2$  excited to high bending vibrational levels of the  $^1\text{B}_1$  state. This has been confirmed by the detection of a LIF signal, at 288.16 and

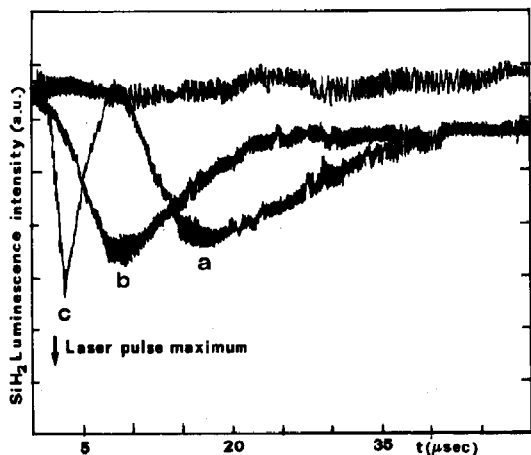


Fig. 2. Time dependence of fragment luminescence at  $p(\text{SiH}_4)=20$  Torr: (a)  $\phi \approx 1.5 \text{ J/cm}^2$ , (b)  $\phi \approx 2.0 \text{ J/cm}^2$ , (c)  $\phi \approx 2.6 \text{ J/cm}^2$ .

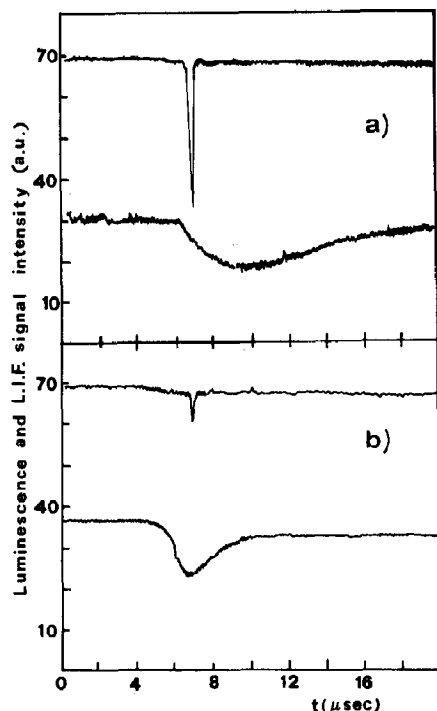


Fig. 4.  $\text{SiH}_2$  spontaneous luminescence signals (lower curves) and  $\text{Si}(^3\text{P})$  LIF signals (upper curves) at two different  $\text{CO}_2$  laser fluences: (a)  $\phi \approx 2.0 \text{ J/cm}^2$ , (b)  $\phi \approx 2.6 \text{ J/cm}^2$ .

at 243.51 nm (fig. 5), following two-photon excitation of  $\text{Si}(^3^1\text{D}_2)$  to  $\text{Si}(^4^1\text{D}_2)$  at  $\text{CO}_2$  laser fluences greater than  $2.5 \text{ J/cm}^2$ .

Keeping in mind the model proposed by Francisco et al. [9] as well as the experiment of Van Zoeren et al. [9], our results are consistent with the following dissociation mechanism for the  $\text{SiH}_2$  radicals formed after IR MPD of  $\text{SiH}_4$ . At a silane pressure of 20 Torr, collision-induced MPD to  $\text{SiH}_2 + \text{H}_2$  takes place at  $\text{CO}_2$  laser fluences greater than  $1 \text{ J/cm}^2$  [5]. The  $\text{SiH}_2$  radicals are formed in the  $^1\text{B}_1$  electronic state and the initial distribution over rovibronic levels depends on the excess energy available during the  $\text{SiH}_4$  dissociation process.

At low  $\text{CO}_2$  laser fluences ( $1 \leq \phi \leq 2.5 \text{ J/cm}^2$ )  $\text{SiH}_2$  can either decay to the ground state emitting the broad chemiluminescence spectrum reported in fig. 1 or dissociate to  $\text{Si}(^3\text{P}) + \text{H}_2$  (figs. 3 and 4). It was shown by Francisco et al. [9] that on symmetry and correlation grounds the  $^1\text{B}_1$  levels cannot dissociate directly to  $\text{Si}(^3\text{P}) + \text{H}_2(^1\Sigma_g^+)$ . It is possible that  $^1\text{B}_1$  levels couple to  $^3\text{B}_1$  states and tunnel through the potential barrier to form  $\text{Si}(^3\text{P}) + \text{H}_2(^1\Sigma_g^+)$ . However,

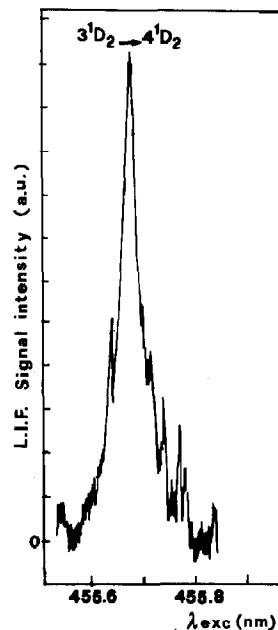


Fig. 5. Two-photon LIF excitation spectrum for  $\text{Si}(^1\text{D}_2)$  atoms after IR MPD of  $\text{SiH}_4$  ( $p = 20 \text{ Torr}$ ) at a  $\text{CO}_2$  laser fluence  $\phi \approx 2.6 \text{ J/cm}^2$ .

the activation energy for this dissociation channel is high ( $44.7 \text{ kcal/mol}$ ) [9] and, as a consequence, only a small number of silicon atoms are formed and nucleate in particles.

As the  $\text{CO}_2$  laser fluence increases, the initial vibrational distribution of  $\text{SiH}_2$  radicals in the  $^1\text{B}_1$  state is shifted towards higher vibrational quantum numbers. In ref. [9] the opening of the  $\text{Si}(^1\text{D}_2) + \text{H}_2(^1\Sigma_g^+)$  dissociation channel is calculated to be  $22.3 \text{ kcal/mol}$  above the origin of the  $\text{SiH}_2(^1\text{B}_1)$  state; Van Zoeren et al. [8] observed the opening of this channel at  $v_2' > 7$ .

Present results indicate that at  $\text{CO}_2$  laser fluences greater than  $2.5 \text{ J/cm}^2$ , a substantial fraction of  $\text{SiH}_2$  radicals is formed in vibronic levels with  $v_2' > 7$  where direct dissociation to  $\text{Si}(^1\text{D}_2) + \text{H}_2(^1\Sigma_g^+)$  is allowed. This is fully confirmed by the sudden detection of a  $\text{Si}(^1\text{D}_2)$  LIF signal, as soon as the  $\text{CO}_2$  laser fluence reaches  $2.5 \text{ J/cm}^2$ , as well as the simultaneous increase in silicon powder production. This last result supports the hypothesis that the channel leading to  $\text{Si}(^1\text{D}_2)$  is more efficient than the predissociation to  $\text{Si}(^3\text{P}) + \text{H}_2$ .

It is worth mentioning that the decrease in the  $\text{Si}(^3\text{P})$  LIF signal as soon as the  $\text{Si}(^1\text{D}_2)$  LIF signal

starts to appear is related to the long radiative lifetime of the Si( $^1D_2$ ) state ( $\tau_{\text{rad}} \approx 370$  s) [16]. We can guess that the Si( $^1D_2$ ) atoms deactivate after reaching the cell walls or form clusters in the gas-phase instead of decaying back to the Si( $^3P$ ) ground state through a forbidden transition.

### Acknowledgement

We wish to thank P. Belardinelli, I. Cenciarelli, M. Nardelli, and G. Schina for technical assistance during the experiments.

### References

- [1] H.E. O'Neal and M.A. Ring, *Chem. Phys. Letters* 107 (1984) 442;  
J.H. Purnell and R. Walsh, *Chem. Phys. Letters* 110 (1984) 330.
- [2] M.E. Coltrin, R.J. Kee and J.A. Miller, *J. Electrochem. Soc.* 131 (1984) 425.
- [3] B.A. Scott, R.M. Placenic and E.E. Simonyi, *Appl. Phys. Letters* 39 (1981) 73.
- [4] B.A. Scott, M.H. Brodsky, D.C. Green, P.B. Kirby, R.M. Placenic and E.E. Simonyi, *Appl. Phys. Letters* 37 (1980) 725.
- [5] E. Borsella and L. Caneve, *Appl. Phys. B* 46 (1988) 347.
- [6] P.A. Longeway and F.W. Lampe, *J. Am. Chem. Soc.* 103 (1981) 6813.
- [7] J.M. Jasinsky and D.R. Estes, *Chem. Phys. Letters* 117 (1985) 495.
- [8] C. Van Zoeren, J.W. Thoman, J.I. Steinfeld and M. Rainbird, *J. Phys. Chem.* 92 (1988) 9.
- [9] J.S. Francisco, R. Barnes and J.W. Thoman, *J. Chem. Phys.* 88 (1988) 2334.
- [10] I.W. Boyd, ed., *Springer series in material science, Vol. 3. Laser processing of thin film and microstructures* (Springer, Berlin, 1987).
- [11] R.W. Cannon, S.C. Danforth, J.H. Flint, J.S. Haggerty and R.A. Marne, *J. Am. Ceram. Soc.* 65 (1981) 324.
- [12] E. Borsella, R. Fantoni and L. Caneve, in: *European Material Research Society Series, Vol. 15. Photon, beam and plasma enhanced processing*, eds. A. Golansky, V.T. Nguyen and F. Krimmel (*Les Edition de Physique, Les Ulis*, 1987) p. 205.
- [13] P.D. Brewer, *Chem. Phys. Letters* 136 (1987) 557.
- [14] S. Bashkin and J.A. Stoner Jr., *Atomic energy levels and Grotian diagrams, Vol. 1* (North-Holland, Amsterdam, 1975).
- [15] I. Oref, *J. Chem. Phys.* 75 (1981) 131.
- [16] J.M. Malville and R.A. Berger, *Planetary Space Sci.* 13 (1965) 1131.